The Oxidation of Rhodium-Platinum

A STUDY BY FIELD ION MICROSCOPY AND IMAGING ATOM PROBE TECHNIQUES

By A. R. McCabe and G. D. W. Smith

Department of Metallurgy and Science of Materials, University of Oxford

The oxidation behaviour of platinum and its alloys at high temperatures is of fundamental importance to its application as both a structural material and a catalyst in a wide range of industrial processes. One of the principal factors determining the efficiency of a catalyst is its surface condition and this in turn depends upon both the initial surface preparation and the changes in surface structure and composition that take place during use. During the manufacture of nitric acid from ammonia a rhodium-platinum catalyst gauze is employed, and under the reaction conditions the surface of the catalyst is altered. The processes involved in this change are not yet fully known, but a study undertaken to provide a more detailed characterisation of the oxide layer formed upon the surface of rhodium-platinum is now reported and may have relevance both to its use as a catalyst in ammonia oxidation and as a structural material.

Rhodium-platinum alloys are widely used as industrial catalysts. One such use is in the manufacture of nitric acid from ammonia, where the catalyst gauze is subjected to strongly oxidising conditions (1). It is known that the catalyst efficiency depends sensitively on the catalyst surface and that extensive changes in both surface structure and composition may take place during use, but a detailed understanding of the processes involved is lacking. Attempts to use electron microprobe analysis to study the composition of the oxide layers on the catalyst surface have been unsuccessful, owing to lack of spatial resolution. Improved resolution may be obtained by field ion microscopy, a technique first reported in this journal by Müller in 1965 (2). In the field ion microscope (FIM) the specimen, in the form of a needle polished to a point with a radius of between about a hundred and a thousand angstroms, is held at a positive potential of up to 30kV relative to an earthed conducting screen, in a chamber which can be evacuated to pressures of approximately 10^{-9} torr before an imaging gas is admitted, see Figure 1. Then the higher field near the tip surface induces polarisation in the image gas atoms, which are attracted and accelerated towards the surface. These atoms lose kinetic energy on collision with the surface, are field ionised to become positive ions which accelerate on approximately radial trajectories towards the detecting screen where they show up as bright spots. As the electric field is greatest above the most prominent atoms in the surface, the pattern of spots corresponds to the atomic arrangement of the specimen surface at a magnification of the order of $\times 10^6$. The principles of field ion microscopy are described in detail in books by Müller and Tsong, and Bowkett and Smith (3).

The FIM technique has since been developed to allow the chemical analysis of individual atoms on specimens by time-of-flight spectrometry, using the so-called "atom probe" method (4). Several versions of the atom probe

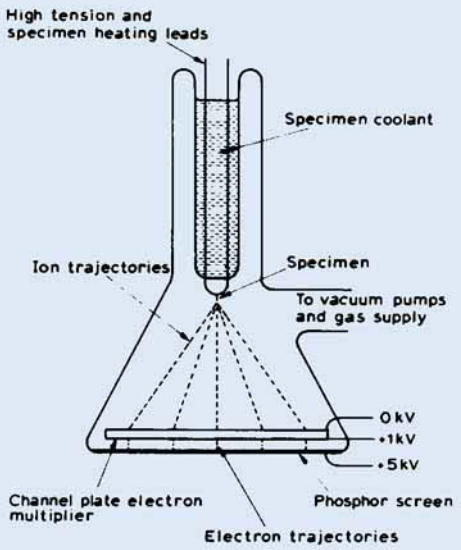

Fig. 1 In the field ion microscope the sharpened specimen is arranged in the vacuum chamber perpendicular to, and pointing towards, the phosphor screen. The specimen is held at a positive potential of up to 30kV and when neon imaging gas is admitted to the chamber, to a pressure of 10^{-5} torr, the gas atoms become ionised and accelerate towards the microscope screen. A channel plate ion detector is placed in the path of the ions, just in front of the screen and converts the incident ion beam to a secondary electron beam before it strikes the phosphor

have been reported but in the present work, we employ the Imaging Atom Probe (IAP) technique, first introduced by Panitz (5). A diagram of this instrument is shown in Figure 2. It consists of a modified FIM, in which the specimen sits at the centre of curvature of a cascade-type double channel plate and screen assembly. On application of a high voltage pulse to the specimen, in addition to the d.c. standing voltage, an oscilloscope sweep is triggered, which records the time of arrival of the desorbed ions at the channel plate detector and produces a time-of-flight spectrum. Probing through the oxide film to the bulk metal below thus provides a large number of such spectra, each of which can be analysed—allowing the construction of concentration profiles through the thin oxide film. "Gated" desorption images can also be produced, displaying visually the spatial distribution of selected chemical species. An account of the operation of the probe can be found in the review article by Panitz (5).

The present FIM/IAP work was undertaken in collaboration with Johnson Matthey with the aim of obtaining a more detailed characterisation of the oxide layers formed on rhodium-platinum alloy surfaces at temperatures up to 800°C.

Experimental Procedure

The specimens for FIM were prepared from 0.13mm diameter high purity 13 weight per cent rhodium-platinum wire (22 atomic per cent rhodium) by electrolytic polishing in molten salt (sodium nitrate-20 per cent sodium chloride) at 440 to 460°C, using a rapid dipping technique developed from that given by Wei and Seidman for platinum-gold alloys (6). A typical rhodium-platinum FIM image, produced in neon at 78K is shown in Figure 3.

After being imaged and field evaporated the

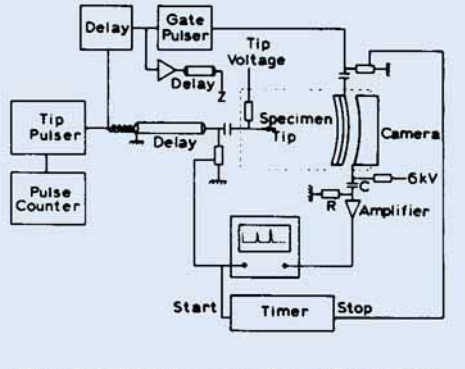

Fig. 2 In the Imaging Atom Probe the tip of the specimen is arranged at the centre of curvature of a cascade-type double channel plate and screen assembly. The application of a high voltage pulse to the tip of the specimen enables the time-of-flight of the desorbed ions to be monitored, by recording the electrical output signal from the channel plate

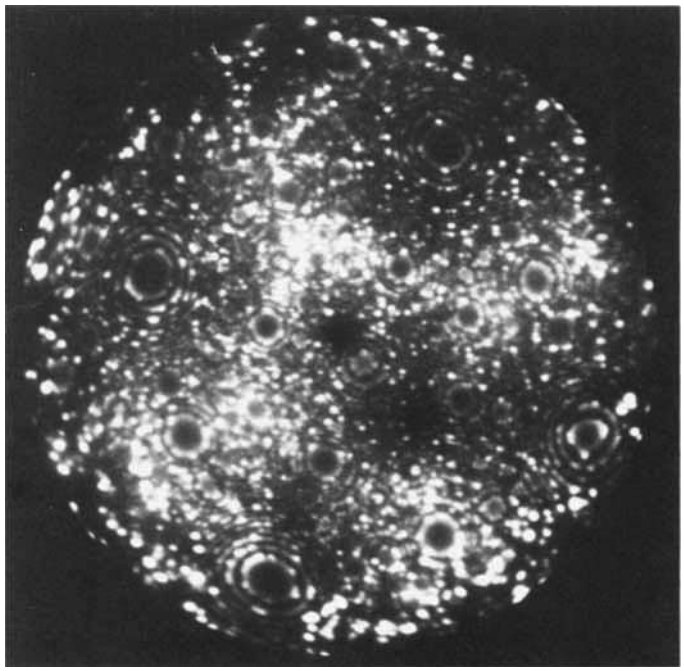

Fig. 3 This neon field ion image of a 13 weight per cent rhodium-platinum wire was obtained at a standing voltage of 12.2 kV and shows a pattern of spots corresponding to the atomic arrangement of the tip of the specimen. Slight irregularities arise in the image because the specimen is an alloy, rather than a pure metal. The overall magnification is approximately 4×10^6

specimens were removed from the microscope and oxidised in an electric tube furnace at temperatures up to 800°C for one hour. The specimens were then air cooled, or in some cases furnace cooled, and were then replaced in the microscope. FIM images were obtained as the surface oxide was stripped off, progressively revealing the metal beneath. The IAP allowed analysis of the layer by layer removal of the surface, thus enabling concentration profiles through the oxide to the bulk metal to be constructed. Further experimental details can be found in reference (7).

Microscopy of Oxide Films

After treatment for one hour at 800°C an oxide film approximately 200 to 300Å thick is obtained. Imaging in the FIM and increasing the standing voltage allows a series of photomicrographs to be obtained as the oxide is stripped off, revealing the metal beneath; such a sequence is illustrated in Figure 4. Initially only the oxide around the (001) substrate metal pole images (Figure 4a) but as the tip blunts, removing some of the oxide film, a larger area of oxide is seen (Figure 4b). Atomic layers of the oxide are seen, in the form of rings around an oxide pole, allowing the collapse of oxide layers to be counted with reference to this pole. After the removal of 40 layers, the image shown in Figure 4c is obtained. When a further 30 layers are stripped off, the thinnest part of the oxide is completely removed, revealing the metal in the region of the (001) pole, Figure 4d. Referring now to the (001) metal pole, stripping off another 16 layers gives rise to the image shown in Figure 4e, while removal of 30 more layers produces the image in Figure 4f. It is interesting to note that the oxide poles and metal poles almost coincide. This is especially clear when looking at the poles on the metal/oxide boundary in Figure 4f, and suggests that the oxide may be growing with an epitaxial relationship to the substrate.

The changes in the specimen profile as the surface layers are removed are shown diagrammatically in Figure 5.

Treatment at 600°C gives a much thinner oxide film, only 30 to 50Å in depth, and provides images clearly showing surface

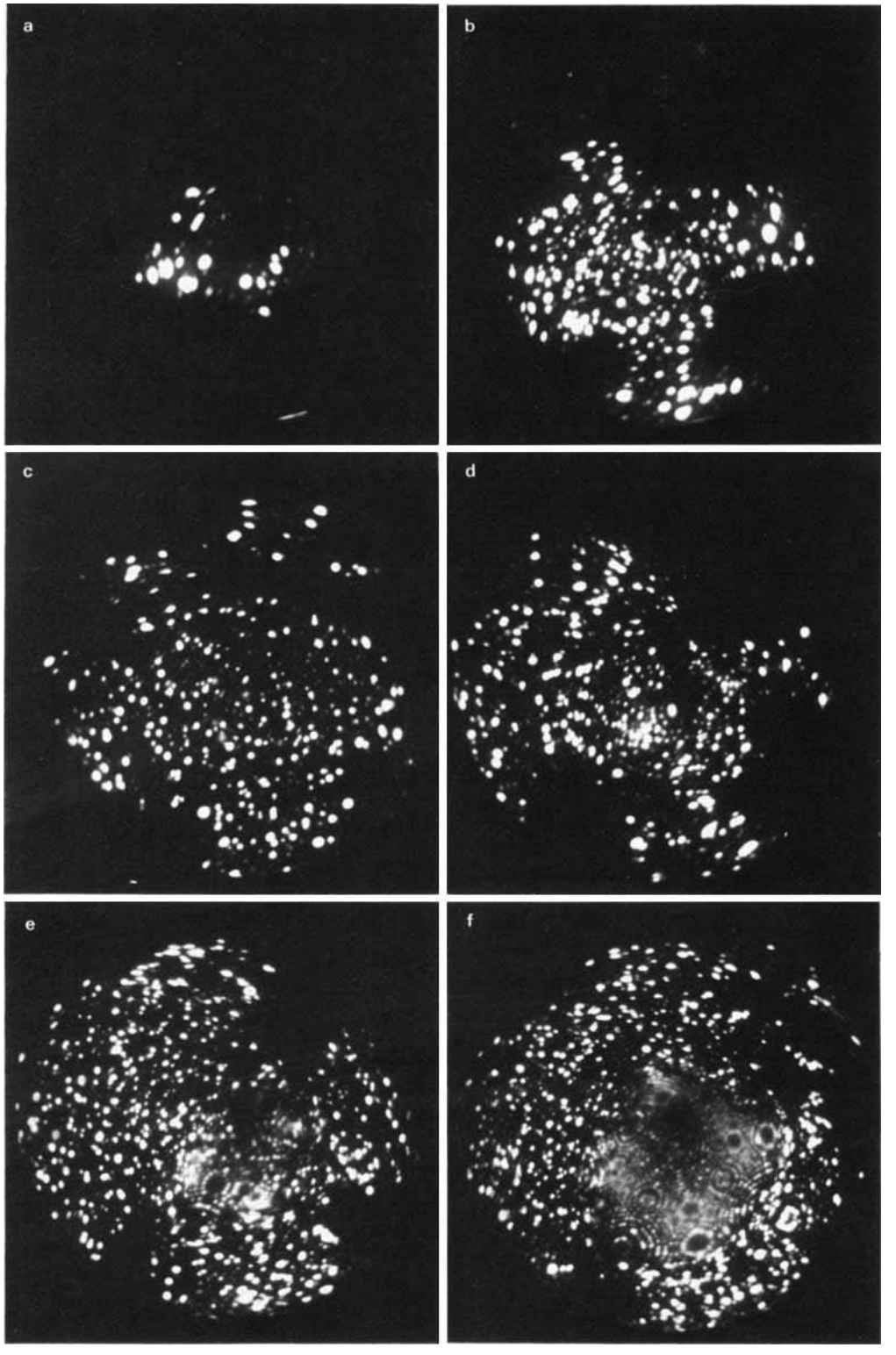
a
b
c
d
e
f

Fig. 4 As the standing voltage is increased the tip of the specimen is progressively stripped off. Here an oxide layer formed at 800°C is shown at various stages of removal. (a) 5.0 kV, (b) 7.5 kV, (c) 8.1 kV, (d) 9.5 kV, (e) 11.5 kV and (f) 13.5 kV. Images (a), (b) and (c) show only the oxide film. In (d), (e) and (f) bulk metal is revealed in the central area of the image as the last of the oxide is removed. The oxide is polycrystalline, and its image is typified by large and rather irregularly arranged spots, with only a few low-index atomic planes visible (in the form of rings of spots). The underlying metal produces a more regular image, consisting of fine, small spots, in which many crystal planes can be identified, as in Figure 3

rearrangements of the substrate, see Figure 6. The effects of thermal faceting are evident, with facets on the central (001) pole and the four peripheral (111) poles. These poles fail to image initially (Figure 6, left), but are later shown to be oxide covered (Figure 6, right) by which stage enough of the oxide has been stripped off to reveal metal on the high index regions around the (001) pole.

Analysis of the Oxide with the Imaging Atom Probe

A time-of-flight spectrum is shown in Figure 7 where the main peaks are identified. From the spectrum the rhodium : rhodium + platinum ratio can be determined. From analysis of a large number of such spectra, a concentration profile through the oxide layer can be constructed. The profile of a specimen oxidised at 800°C is shown in Figure 8 and clearly shows rhodium enrichment of the oxide. The metal : oxygen atom ratio in the oxide layer is estimated to be 1 : 1.8. A similar profile for 600°C indicates that at this temperature the outer surface of the oxide is not so enriched in rhodium as the bulk of the oxide—possibly due to the redeposition of PtO_2 from the vapour phase onto the oxide surface; PtO_2 being the most volatile oxide constituent below about 1100°C. This was confirmed by slowly cooling in a furnace some of the specimens oxidised at 600°C. Under these conditions, the increased level of platinum in the outer layers of the oxide was more noticeable than for specimens which had been removed from the furnace and rapidly air cooled. It should be noted that the bulk metal beneath the oxide layer does not show a detectable rhodium depleted region. This suggests that the main process by which rhodium build-up in the oxide layer takes place may be the loss of platinum by volatilisation, as PtO_2, from the oxide surface.

Discussion

It is believed that this is the first time that FIM/IAP techniques have been applied to the study of an alloy system used as a practical industrial catalyst. The results show a strong enrichment of rhodium in the surface oxide phase, in agreement with recent Auger Electron Spectroscopy results reported from the Ford Motor Company laboratories, Dearborn (8). However, the presence of some platinum in the oxide layer may be a factor of great significance.

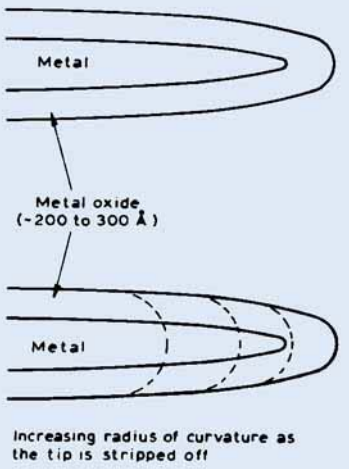

Fig. 5 Initially the end of the specimen featured in Figure 4 is completely covered by an oxide layer approximately 200 to 300Å thick but as the field evaporation process proceeds this layer is progressively removed from the tip exposing a core of metal, which is surrounded by a shell of residual oxide

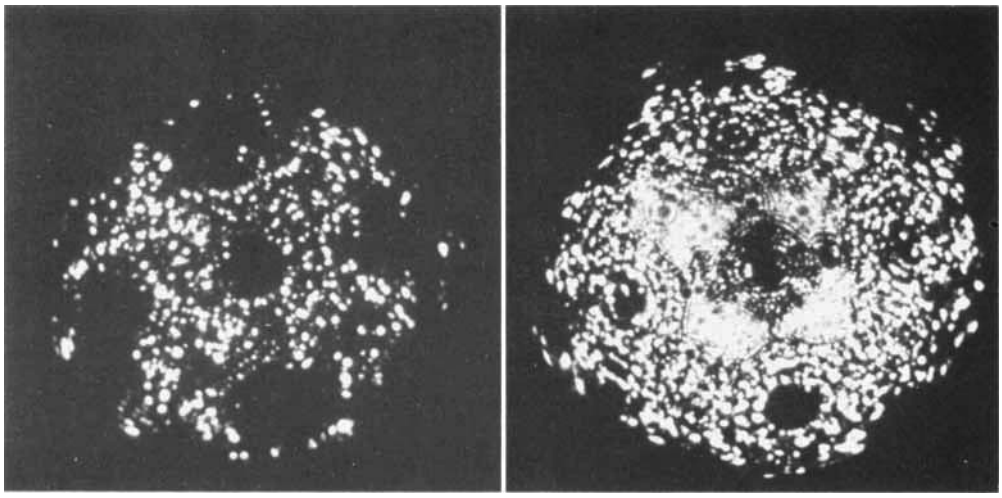

Fig. 6 Treatment at 600°C results in a thinner oxide layer than that produced at 800°C and shown in Figure 4. However, evaporation through the thinner oxide layer shows thermal faceting on (001) and (111) poles. These poles are not imaged initially at 12.0 kV (left), but at 15.75 kV (right) sufficient oxide has been removed to reveal metal around the (001) pole

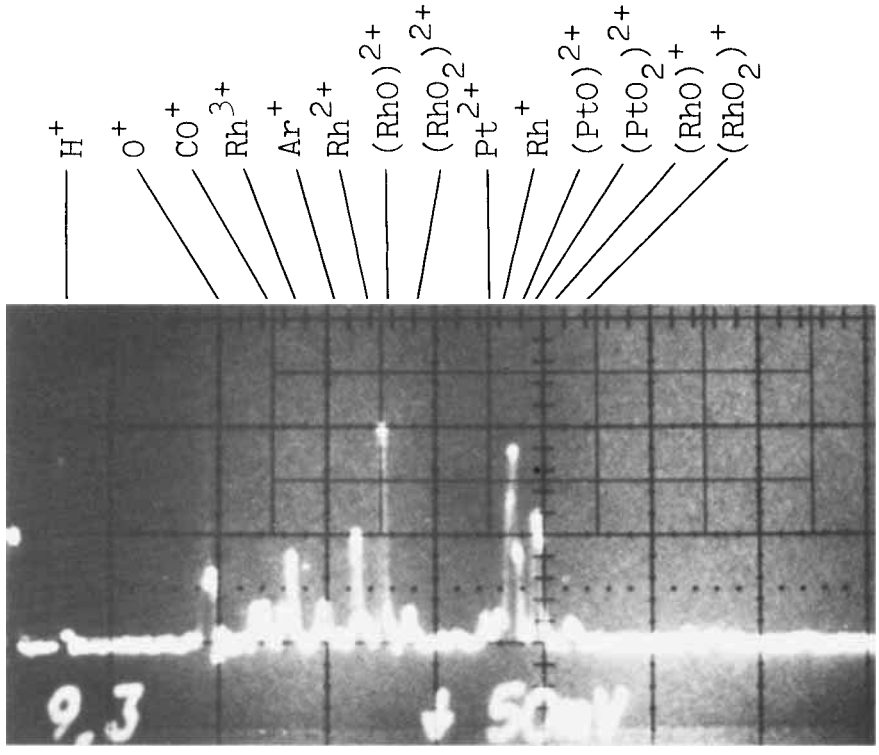

Fig. 7 This typical time-of-flight spectrum from an oxide film layer formed at 600°C has the main peaks identified. From analysis of many such spectra a concentration profile through the oxide layer may be constructed

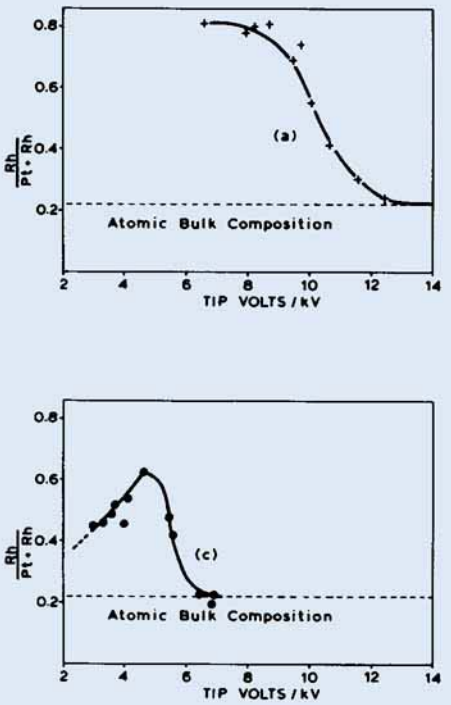

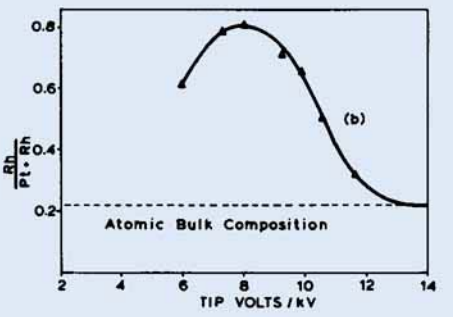

Fig. 8 Concentration profiles through oxide layers formed in air at:
(a) 800°C for 1 hour then air cooled
(b) 600°C for 1 hour then air cooled
(c) 600°C for 1 hour then slowly furnace cooled.
Low tip voltages correspond to the outer regions of the oxide layers, thus at 800°C there is rhodium enrichment throughout the oxide; the outer surface of the 600°C air cooled oxide layer is not as rhodium enriched as the bulk of the oxide, while the slow cooled 600°C layer has a markedly higher platinum content on the outer surface of the oxide

It is known that the stable oxide of rhodium, Rh_2O_3, is catalytically inactive, while the stable oxide of platinum, PtO_2 is very active (9). The present work demonstrates that the proportion of platinum atoms in the outer layers of the oxide film on rhodium-platinum alloys is sensitively dependent on the thermal history of the specimen. This is a completely novel result. Some of the effects of various proprietary surface pre-treatments of catalyst gauzes, designed to raise their initial activity, may possibly be understood in terms of their effectiveness in decreasing the rhodium: platinum ratio at the surface of the oxide layer. The main function of the rhodium could then be considered in terms of its overall stabilising effect on the oxide film structure. Further work is now being undertaken in collaboration with Johnson Matthey Group Research Centre and will include the study of hydrogen reduction cycles, poisoning and the exposure of various catalyst systems to different gas environments.

Acknowledgements

The provision of materials, and advice by Dr. D. T. Thompson and Mr. A. S. Pratt, of the Johnson Matthey Group Research Centre are gratefully acknowledged.

References

1 J. A. Busby, A. G. Knapton and A. E. R. Budd, Proc. Fertiliser Soc., 1978, No. 169, 3–37
2 E. W. Müller, *Platinum Metals Rev.*, 1965, **9**, (3), 84
3 E. W. Müller and T. T. Tsong, "Field Ion Microscopy", Elsevier, 1969; K. M. Bowkett and D. A. Smith, "Field Ion Microscopy", North Holland, 1970
4 E. W. Müller, J. A. Panitz and S. B. McLane, *Rev. Sci. Instrum.*, 1968, **39**, (1), 83
5 J. A. Panitz, *Prog. Surf. Sci.*, 1978, **8**, (6), 219
6 C. Y. Wei and D. N. Seidman, *Radiat. Eff.*, 1977, **32**, (3/4), 229
7 A. R. McCabe, Metallurgy Part II Thesis, Oxford University, June 1982
8 W. B. Williamson, H. S. Gandhi, P. Wynblatt, T. J. Truex and R. C. Ku, AIChE Symposium Series, 1980, **76**, (201), 212
9 J. E. Philpott, *Platinum Metals Rev.*, 1971, **15**, (2), 52